

Edge modes in finite-size systems with different edge terminals

Huiping Wang(王会平), Li Ren(任莉), Xiuli Zhang(张修丽), and Liguo Qin(秦立国)

Citation: Chin. Phys. B, 2024, 33 (**10**): 107302. DOI: 10.1088/1674-1056/ad6a05
Journal homepage: http://cpb.iphy.ac.cn; http://iopscience.iop.org/cpb

What follows is a list of articles you may be interested in

Quantum confinement of carriers in the type-I quantum wells structure

Xinxin Li(李欣欣), Zhen Deng(邓震), Yang Jiang(江洋), Chunhua Du(杜春花), Haiqiang Jia(贾海强), Wenxin Wang(王文新), and Hong Chen(陈弘)
Chin. Phys. B, 2024, 33 (**9**): 097301. DOI: 10.1088/1674-1056/ad5d99

Topological superconductors with spin-triplet pairings and Majorana Fermi arcs

Shi Huang(黄石) and Xi Luo(罗熙)
Chin. Phys. B, 2024, 33 (**8**): 087301. DOI: 10.1088/1674-1056/ad462f

Gate-field control of valley polarization in valleytronics

Ting-Ting Zhang(张婷婷), Yilin Han(韩依琳), Run-Wu Zhang(张闰午), and Zhi-Ming Yu(余智明)
Chin. Phys. B, 2024, 33 (**6**): 067303. DOI: 10.1088/1674-1056/ad401a

Edge states enhanced by long-range hopping: An analytical study

Huiping Wang(王会平), Li Ren(任莉), Liguo Qin(秦立国), and Yueyin Qiu(邱岳寅)
Chin. Phys. B, 2021, 30 (**10**): 107301. DOI: 10.1088/1674-1056/abe9a5

Identifying anomalous Floquet edge modes via bulk-edge correspondence

Huanyu Wang(王寰宇), Wuming Liu(刘伍明)
Chin. Phys. B, 2020, 29 (**4**): 047301. DOI: 10.1088/1674-1056/ab6dcb

---

Edge modes in finite-size systems with different edge terminals

Huiping Wang(王会平)[†], Li Ren(任莉), Xiuli Zhang(张修丽), and Liguo Qin(秦立国)

School of Mathematics, Physics and Statistics, Shanghai University of Engineering Science, Shanghai 201620, *China*

(Received 27 March 2024; revised manuscript received 13 July 2024; accepted manuscript online 1 August 2024)

We investigate the behavior of edge modes in the presence of different edge terminations and long-range (LR) hopping. Here, we mainly focus on such model crystals with two different types of structures (type I: "$\cdots$–P–Q–P–Q–$\cdots$" and type II: "$\cdots = P$–$Q = P$–$Q = \cdots$"), where P and Q represent crystal lines (CLs), while the symbols "–" and "=" denote the distance between the nearest neighbor (NN) CLs. Based on the lattice model Hamiltonian with LR hopping, the existence of edge modes is determined analytically by using the transfer matrix method (TMM) when different edge terminals are taken into consideration. Our findings are consistent with the numerical results obtained by the exact diagonalization method. We also notice that edge modes can exhibit different behaviors under different edge terminals. Our result is helpful in solving novel edge modes in honeycomb crystalline graphene and transition metal dichalcogenides with different edge terminals.

Keywords: edge modes, long-range hopping, different edge terminals

PACS: 73.20.At, 61.50.Ah, 73.22.Dj, 02.10.Yn **DOI:** 10.1088/1674-1056/ad6a05

1. Introduction

In the field of topological states of matter, it is widely assumed that their existence remains unaffected by specific details, except for the band topology. This fundamental principle holds true for both quantum Hall effects[1–3] and quantum spin Hall effects.[4,5] However, theoretical predictions have highlighted the significance of the boundaries in topological crystalline insulators.[6,7] The reason is that the topological invariant is dependent on the choice of unit cell, which subsequently determines the geometry of the edges. Moreover, the edges of two-dimensional (2D) materials exhibit significant functionalities and distinct properties owing to the presence of dangling chemical bonds and the loss of symmetry. It has been reported that the electronic and magnetic properties of honeycomb crystalline graphene and transition metal dichalcogenides show a strong dependence on the atomic configurations on the edges.[8–24] These interesting physical phenomena are mainly governed by Hamiltonians with short-range terms. However, the addition of long-range (LR) hopping amplitudes is important, because they are ubiquitous in real systems and their role can be crucial.[25–27] In previous theoretical studies, many interesting and unusual phenomena have been discussed in systems with LR interactions, which arise from the violation of locality.[28–31]

Motivated by these ideas, we study the behavior of edge modes in LR interacting systems with different edge terminals. It is natural to ask how different edge terminals and LR terms influence edge modes. This paper aims to explore the conditions for the existence of edge modes in the LR interacting systems with different edge terminals in terms of the transfer matrix method (TMM). It is known that an infinite n-dimensional crystal comprises an infinite number of periodically arranged parallel $(n-1)$-dimensional crystals through coupling. For the purpose of discussion, we consider a 2D crystal as an example. The $(n-1)$-dimensional crystal corresponds to the crystal line (CL) when n equals 2. In this study, our primary focus lies on model crystals with two distinct structural types (type I "$\cdots$–P–Q–P–Q–$\cdots$" and type II "$\cdots = P$–$Q = P$–$Q = \cdots$"), where P and Q represent CLs, while the symbols "–" and "=" denote the distance between the nearest neighbor (NN) CLs (see Figs. 1(a) and 1(b)). For model crystals with type I (II), the structures of edge terminals have two cases: P–Q–P–Q–$\cdots$–P–Q ($P \leftrightarrow Q$) and P–Q–P–Q–$\cdots$–P–Q–P ($P \leftrightarrow P$) (P–$Q = P$–$Q = \cdots = P$–Q ($P \Leftrightarrow Q$) and P–$Q = P$–Q–$\cdots = P$–$Q = P$ ($P \Leftrightarrow P$)) (see Figs. 1(c)–1(f)). It is noteworthy that our approach is also applicable to other structural type crystals, such as P–Q–R–P–Q–R–$\cdots$–P–Q–R.

In this work, we perform an analytical investigation into the behavior of edge modes in LR interacting systems with different edge terminals via TMM. For model crystals exhibiting two distinct structural types, we analytically determine the conditions for the presence of edge modes across different edge terminals. The analysis encompasses the LR hopping among CLs, as well as all possible neighbor hoppings within each CL. Our results are substantiated by numerical calculations performed for specific parameter choices. We find that edge modes can demonstrate distinct behaviors when different edge terminals are taken into account.

[†]Corresponding author. E-mail: hp_wang@fudan.edu.cn

© 2024 Chinese Physical Society and IOP Publishing Ltd

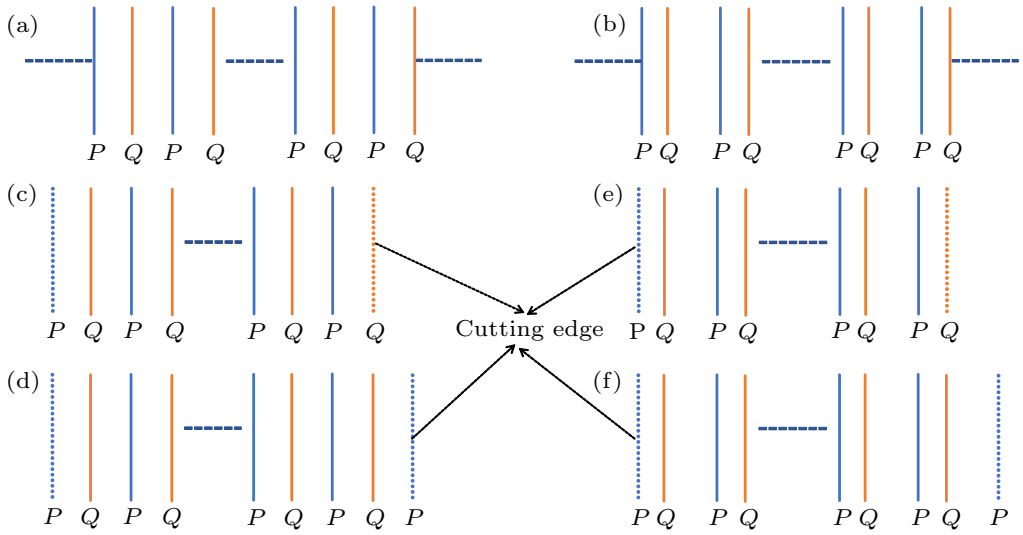


Fig. 1. Two distinct structural types of infinite crystals: (a) type I "$\cdots$–*P*–*Q*–*P*–*Q*–$\cdots$" and (b) type II "$\cdots = P$–$Q = P$–$Q = \cdots$". The structures with different edge terminals for type I in (c) with $P \leftrightarrow Q$ and (e) with $P \leftrightarrow P$ and type II in (d) with $P \Leftrightarrow Q$ and (f) with $P \Leftrightarrow P$.

Prior to commencing the ensuing discussion, we shall initially provide a precise definition of "edge mode". The edge mode is characterized by its propagation along the cutting boundary direction, with its amplitude exponentially decaying at the distance perpendicular to the cutting boundary. By employing the transfer matrix language, one can derive the exponential decay relation for an edge mode as follows:

$$\begin{cases} |\psi_{i+1}/\psi_i| = \delta = \mathrm{e}^{-\gamma a} < 1, \\ a > 0, \ \ \gamma > 0, \ \ i \geq 1, \end{cases} \tag{1}$$

where γ is a decay rate and a is the distance between the 1NN CLs. When $\delta = 1$ ($\gamma = 0$), ψ_i corresponds to the extended mode and must be associated with the bulk mode.

2. Transfer matrix method

In order to gain a more comprehensive understanding the behavior of edge modes in the presence of different edge terminations and the LR hopping, we will introduce our TMM by using an example of the one-dimensional (1D) finite-size single-orbital atomic chain model. Taking into account the LR coupling, the model Hamiltonian can read

$$H_0 = \sum_{i=1}^{n'} \left\{ \varepsilon \psi_i^\dagger \psi_i + \sum_{j=1}^{m'} [t_j \psi_i^\dagger \psi_{i+j} + \cdots + \text{h.c.}] \right\}, \tag{2}$$

with

$$\psi_i = 0 : i < 1, \quad i > n'; \quad m' \ll n'.$$

Here ψ_i is the second quantized Fermionic wave function of the electron mode in the i^{th} crystal point. t_j represents the hopping parameter from the different crystal points. Due to the original infinite crystal with the geometric reflection symmetry for each crystal point, the quantum dynamical equations (QDEs) of Eq. (2) in the bulk and boundary layers are obtained as

$$E_1 \psi_i = \sum_{j=1}^{m'} t_j (\psi_{i-j} + \psi_{i+j}), \tag{3}$$

where $E_1 = E - \varepsilon$, E is the eigenenergy of electron waves propagating in the crystals and ε is the on-site energy. By some simple calculations, one can rewrite Eq. (3) in the following matrix form:

$$\begin{cases} \Theta_{n+m'} = \Theta_{n+m'-1} T_{2m' \times 2m'}, \\ n = 1, 2, 3, \ldots, n' - m', \end{cases} \tag{4}$$

where

$$T_{2m' \times 2m'} = \begin{pmatrix} T_{11} & T_{12} \\ T_{21} & T_{22} \end{pmatrix},$$

$T_{11}^{\mathrm{T}} = \{b_1, b_2, \ldots, b_{m'-1}, b_{m'}, b_{m'-1}, \ldots, b_2, b_1\}$ with $\{b_{m'} = E_1/t_{m'}, b_i = -t_{m'-i}/t_{m'} : i = 1, 2, \ldots, m'-2, m'-1\}, T_{21} = -1$, T_{12} is a $(2m'-1) \times (2m'-1)$ identity matrix, T_{22} is a $1 \times (2m'-1)$ zero matrix and $\Theta_n = \{\psi_n, \psi_{n-1}, \ldots, \psi_{n-2m'+2}, \psi_{n-2m'+1}\}$. From Eq. (4), we can clearly see that the transfer matrix in the bulk is the same as that in the boundary layers. We notice that if λ is the eigenvalue of the transfer matrix $T_{2m' \times 2m'}$, $1/\lambda^*$ is found to be also its eigenvalue. The key quantity of this approach is the composite transfer matrix $T_{2m' \times 2m'}$, which encapsulates essential information regarding the bulk projected band structure, the eigenenergies of edge modes, their character, and decay lengths. The rest of this section will elucidate these details derived from $T_{2m' \times 2m'}$. As is well known, a Jordan form $J_{2m' \times 2m'}$ of a square matrix $T_{2m' \times 2m'}$ can be obtained through a similarity transformation $U_{2m' \times 2m'}$, where the specific expressions of $J_{2m' \times 2m'} = \sum_{i=1}^{2\alpha} J_{n_i}(\lambda_i)$ and $U_{2m' \times 2m'}$ are given.[32,33] Meanwhile, we also note that prior work[34] takes no consideration of the degeneracy of eigenvalues of the transfer matrix. By

means of TMM,[34–37] Eq. (4) can be expressed as

$$\begin{cases} \Theta_{n+m'} = \Omega_0 U_{2m'\times 2m'} \sum_{i=1}^{2\alpha} J_{n_i}^n(\lambda_i) U_{2m'\times 2m'}^{-1} \\ \qquad\quad = (N_1, N_2, \ldots, N_{2m'}) \sum_{i=1}^{2\alpha} J_{n_i}^n(\lambda_i) U_{2m'\times 2m'}^{-1}, \\ \Omega_0 = \{\psi_{m'}, \psi_{m'-1}, \ldots, \psi_1, 0, 0, \ldots, 0, 0\}, \\ n = 1, 2, \ldots, n'-m', \end{cases} \tag{5}$$

here $\{N_i = U_{1i}\psi_{m'} + U_{2i}\psi_{m'-1} + \cdots + U_{(m'-1)i}\psi_2 + U_{m'i}\psi_1 : i = 1, 2, \ldots, 2m'\}$. $n_1 + n_2 + \cdots + n_{2\alpha} = 2m'$, where $\alpha \leq m'$ and $\{\lambda_i : i = 1, 2, \ldots, 2\alpha\}$ are the eigenvalues of $T_{2m'\times 2m'}$. For the sake of the subsequent discussion and without loss of generality, we make such an assumption $\{|\lambda_i| \geq 1, |\lambda_{i+\alpha}| \leq 1, \lambda_i\lambda_{i+\alpha} = 1 : i = 1, 2, \ldots, \alpha-1, \alpha\}$ and $|\lambda_1|$ is the largest. Once one of $\{\lambda_i : i = 1, 2, \ldots, 2\alpha\}$ is equal to one, corresponding to extended modes which we do not focus on. Thus, we need to consider $\{|\lambda_i| > 1, |\lambda_{i+\alpha}| < 1, \lambda_i\lambda_{i+\alpha} = 1 : i = 1, 2, \ldots, \alpha-1, \alpha\}$. For the 1D finite-size single-orbital atomic chain, the following two conditions have to be fulfilled in order to obtain physically meaningful and normalizable solutions:

1) When one of the left and right boundary conditions is fulfilled, we have to impose the restriction $\{N_j = 0 : j = 1, 2, \ldots, m'\}$ because the left and right boundaries are identical for the 1D finite-size single-orbital atomic chain.

2) When both left and right boundary conditions are satisfied, we will examine two scenarios, that is, the eigenvalue $|\lambda_1|$ is degenerate and nondegenerate. We first discuss the case where $|\lambda_1|$ is nondegenerate. For the 1D finite-size single-orbital atomic chain, one can obtain by means of the right boundary conditions and Eq. (5)

$$\begin{cases} 0 = \left\{\sum_{i=1}^{m'-1} \frac{b_i}{\lambda_1^i} + \frac{1}{\lambda_1^{m'}} - b_{m'} + \sum_{i=0}^{\delta} \lambda_1^i b_i\right\} N_1, \\ b_0 = 0; \quad \delta = 0, 1, 2, \ldots, \quad m'-1. \end{cases} \tag{6}$$

In terms of Eq. (6), there are no edge modes in the 1D finite-size single-orbital atomic chain. Next, the ongoing discussion will continue to focus on the scenario in which $|\lambda_1|$ is degenerate and the degeneracy is n_i. Through the use of Eq. (5) and the right boundary conditions, we can arrive at

$$\begin{cases} 0 = \left\{\sum_{i=1}^{m'-1} \frac{b_i}{\lambda_1^i} + \frac{1}{\lambda_1^{m'}} - b_{m'} + \sum_{i=0}^{\delta} \lambda_1^i b_i\right\} M, \\ M = \sum_{j=1}^{n_i} \sum_{k=j}^{n_i} l_{k-1} U_{k,1}^{-1} N_j, \quad l_{k-1} = \frac{1}{\lambda_1^{k-1}} C_{n'-m'-\delta}^{k-1}, \\ b_0 = 0; \quad \delta = 0, 1, 2, \ldots, \quad m'-1. \end{cases} \tag{7}$$

We can find that no edge modes exist in the 1D finite-size single-orbital atomic chain via Eq. (7).

3. Model Hamiltonian with $P \leftrightarrow Q$

In this section, we discuss such model crystals composed of two different CLs: P and Q. Here we only focus on such a finite-size crystal with $P \leftrightarrow Q$ because the discussion for the $P \leftrightarrow P$ case will be similar. For a finite-size crystal, each of its CLs is still a crystal with the lower dimensionality. We can perform the Fourier transformation in each CL, resulting from the wave vector $\boldsymbol{k}_{\parallel}$ being a good quantum number along the boundary. To enhance clarity in writing, the omission of $\boldsymbol{k}_{\parallel}$ is implemented. Taking into account the LR coupling from rNN CLs where we temporarily assume that r is an even number to facilitate theoretical demonstration and analysis, our effective model Hamiltonian reads via the diagonal representation of each CL Hamiltonian

$$\begin{aligned} H_0 = \sum_{i=1}^{n'} \Big\{ & \Psi_{2i-1}^{\dagger} \varepsilon_{n\times n}^{(P)} \Psi_{2i-1} + \Phi_{2i}^{\dagger} \varepsilon_{m\times m}^{(Q)} \Phi_{2i} \\ & + \sum_{j=1}^{m'} \{\Phi_{2i}^{\dagger} B_{m\times m}^{(2j)} [\Phi_{2i+2j} + \Phi_{2i-2j}] \\ & + \Psi_{2i-1}^{\dagger} A_{n\times n}^{(2j)} [\Psi_{2i-1+2j} + \Psi_{2i-1-2j}] \\ & + \{\Psi_{2i-1}^{\dagger} F_{n\times m}^{(2j-1)} [\Phi_{2i-1+2j-1} + \Phi_{2i-1-(2j-1)}] \\ & + \text{h.c.}\}\} \Big\}, \end{aligned} \tag{8}$$

here $\{\Psi_{2i-1} = \Phi_{2i} = 0 : i < 1, \quad i > n'\}$, $\Psi_{2i-1}^{\mathrm{T}} = \{\psi_{2i-1}^{(1)}, \psi_{2i-1}^{(2)}, \ldots, \psi_{2i-1}^{(n)}\}$, $\Phi_{2i}^{\mathrm{T}} = \{\phi_{2i}^{(1)}, \phi_{2i}^{(2)}, \ldots, \phi_{2i}^{(m)}\}$, $\varepsilon_{l_\alpha\times l_\alpha}^{(\alpha)} = \mathrm{diag}(\varepsilon_1^\alpha, \varepsilon_2^\alpha, \ldots, \varepsilon_{l_\alpha}^\alpha)$, where $l_{P(Q)} = n$ (m) when $\alpha = P$ (Q) and the CLs P and Q have n and m modes respectively where n and m can be equal or unequal as well as $m' = r/2$. $\{F_{n\times m}^{(2j-1)}, A_{n\times n}^{(2j)}, B_{m\times m}^{(2j)}\}$ denote the hopping matrices from the different CLs, $\{\varepsilon_i^\alpha : i = 1, 2, \ldots, l_\alpha\}$ are the energies of renormalized eigenmodes in each CL, the matrix elements of $\{\varepsilon_{n\times n}^{(P)}, \varepsilon_{m\times m}^{(Q)}, F_{n\times m}^{(2j-1)}, A_{n\times n}^{(2j)}, B_{m\times m}^{(2j)}\}$ consist of the hopping parameters and $\overrightarrow{k}_{\parallel}$. $\{\psi_{2i-1}^{(\alpha)} : \alpha = 1, 2, \ldots, n\}$ $(\{\phi_{2i}^{(\beta)} : \beta = 1, 2, \ldots, m\})$ is the second quantization Fermi wave function of the α^{th} (β^{th}) electron mode in the $(2i-1)^{\mathrm{th}}$ $((2i)^{\mathrm{th}})$ CL. The assumption here is that $m' \ll n'$ and each unit cell in each CL contains multiple atoms (which may be different), with each atom potentially contributing multiple nonidentical atomic orbits. As a result, the proposed model Hamiltonian can be applied to some real materials. QDEs from Eq. (8) in both bulk and boundary layers can be expressed as

$$\begin{cases} E_{n\times n}^{(P)} \Psi_{2i-1} = \sum_{j=1}^{m'} \{F_{n\times m}^{(2j-1)} \blacktriangle_{2j-1} \Phi_{2i-1} + A_{n\times n}^{(2j)} \Delta_{2j} \Psi_{2i-1}\}, \\ E_{m\times m}^{(Q)} \Phi_{2i} = \sum_{j=1}^{m'} \{(F_{n\times m}^{(2j-1)})^{\dagger} \blacktriangle_{2j-1} \Psi_{2i} + B_{m\times m}^{(2j)} \Delta_{2j} \Phi_{2i}\}, \\ \blacktriangle_{2j-1} \Psi_{2i} = \Psi_{2i-(2j-1)} + \Psi_{2i+2j-1}, \\ \Delta_{2j} \Psi_{2i-1} = \Psi_{2i-1-2j} + \Psi_{2i-1+2j}, \\ \blacktriangle_{2j-1} \Phi_{2i-1} = \Phi_{2i-1-(2j-1)} + \Phi_{2i-1+2j-1}, \\ \Delta_{2j} \Phi_{2i} = \Phi_{2i-2j} + \Phi_{2i+2j}, \\ E_{l_\alpha\times l_\alpha}^{(\alpha)} = \mathrm{diag}\{E_1^\alpha, E_2^\alpha, \ldots, E_{l_\alpha}^\alpha\}, \\ E_\tau^\alpha = E - \varepsilon_\tau^\alpha : \tau = 1, 2, \ldots, l_\alpha, \end{cases} \tag{9}$$

where E is the eigenenergy of electron waves propagating in the crystals. Previous studies have investigated edge modes under semi-infinite boundary conditions by employing lattice model Hamiltonian with the LR coupling among CLs and all possible neighbor hoppings within each CL and found the presence of edge modes, resulting from the transfer matrix in the bulk different from that in the boundary layers.[32,33] However, in practical materials, their size is always finite. Thus, this paper aims to explore the influence of different edge terminals on edge modes in LR interacting systems. To enhance the acceptability of our conclusion, we will begin by considering a specific instance where m and n are both equal to 1, and subsequently extend our analysis to encompass the general case.

We first notice the absence of edge modes by careful analytical calculations when only the hopping from 1NN CPs is taken into account. To validate our findings, we present a finite 2D square lattice in Fig. 2(a), featuring two distinct sublattices. As the y-direction extends infinitely, Fourier transformation can be employed on wave functions for P and Q sublattices. When we consider the hopping from 1NN CLs, QDEs are expressed in the $\{i,k_y\}$ representation by a set of Fermion operators $\{\psi^{(1)}_{2i-1,}(k_y),\phi^{(1)}_{2i}(k_y): i=1,2,3,\ldots,n' \text{ and } n'\gg 1\}$

$$\begin{cases} E_1^P\psi^{(1)}_{2i-1}=F^{(1)}_{11}(\phi^{(1)}_{2i}+\phi^{(1)}_{2i-2}),\\ E_1^Q\phi^{(1)}_{2i}=F^{(1)}_{11}(\psi^{(1)}_{2i+1}+\psi^{(1)}_{2i-1}), \end{cases} \tag{10}$$

with

$$\begin{cases} E_1^\alpha=E-\varepsilon_1^\alpha,\ \ \alpha=P,Q,\\ F^{(1)}_{11}=2t_1\cos(k_y a),\\ \psi^{(1)}_{2i-1}=\phi^{(1)}_{2i}=0,\ \ i\le 0 \text{ and } i>n', \end{cases}$$

$F^{(1)}_{11}$ represents the coupling from 1NN CLs, ε_1^α is the on-site energy, t_1 is the hopping parameter and $\{\varepsilon_1^\alpha,F^{(1)}_{11}\}$ are real. By the exact diagonalization method, it is noteworthy that no edge modes can appear in the finite-size crystal with $P\leftrightarrow Q$ (see Fig. 2(b)), which is completely consistent with our analytical discussion. Moreover, to make our presentation more convincing, we also calculate such a finite-size crystal with $P\leftrightarrow P$ in detail, which is still compatible with the numerical conclusion (see Fig. 2(c)).

The significance lies in the addition of LR hopping amplitudes because they are ubiquitous in real systems and their effects can be critical.[25–27] The problem worth investigating is whether there exist edge modes when the LR coupling is taken into account under the condition of $n=m=1$, and if so, then what are the necessary conditions for their existence? In our effort to answer this question, we will continue our discussion. Next, when $\{F^{(2\alpha-1)}_{11}\neq 0, A^{(2\alpha)}_{11}\neq 0, B^{(2\alpha)}_{11}\neq 0: \alpha=1,2,\ldots,m'\}$ and $F^{(2\alpha+1)}_{11}=A^{(2\alpha+2)}_{11}=B^{(2\alpha+2)}_{11}=0:\alpha=m'+1,m'+2,\ldots\}$, one can transform Eq. (9) into the following matrix form after complex mathematical calculations:

$$\begin{cases} \Theta^{(P)}_{l+8m'-2}=\Theta^{(P)}_{l+8m'-4}T_{4m'\times 4m'},\Theta^{(Q)}_{l+8m'-1}\\ \qquad\qquad =\Theta^{(Q)}_{l+8m'-3}T_{4m'\times 4m'},\\ \Theta^{(P)}_{8m'-3}=\Omega_0\prod_{\beta=1}^{2m'}S^{(\beta)}_{4m'\times 4m'},\\ \Theta^{(Q)}_{8m'-2}=\Omega_0\prod_{\beta=1}^{2m'}R^{(\beta)}_{4m'\times 4m'},\\ T_{4m'\times 4m'}=\begin{pmatrix} T_{11} & T_{12}\\ T_{21} & T_{22}\end{pmatrix},\ \ l=1,3,\ldots,n'-8m', \end{cases} \tag{11}$$

here

$$T_{11}^{\mathrm{T}}=\{b_1,b_2,\ldots,b_{2m'-1},b_{2m'},b_{2m'-1},\ldots,b_2,b_1\},$$

T_{12} is a $(4m'-1)\times(4m'-1)$ identity matrix, T_{22} is a $1\times(4m'-1)$ zero matrix, $T_{21}=-1$, $\{b_i: i=1,2,\ldots,2m'-1,2m'\}$ and the matrix elements in $\{T_{4m'\times 4m'},S^{(\beta)}_{4m'\times 4m'},R^{(\beta)}_{4m'\times 4m'}\}$ are arbitrary complex functions of $\{F^{(2\alpha-1)}_{11},A^{(2\alpha)}_{11},B^{(2\alpha)}_{11}\}$ and $\{E_1^P,E_1^Q\}$ as well as $\Theta^{(P)}_{l+8m'-2}=\{\psi^{(1)}_{l+8m'-2},\psi^{(1)}_{l+8m'-4},\cdots\psi^{(1)}_{l+4m'+1},\ \psi^{(1)}_{l+4m'-1}\}$, $\Theta^{(Q)}_{l+8m'-1}=\{\phi^{(1)}_{l+8m'-1},\phi^{(1)}_{l+8m'-3},\ldots,\phi^{(1)}_{l+4m'+2},\phi^{(1)}_{l+4m'}\}$, $\Omega_0=\{\phi^{(1)}_{2m'},\psi^{(1)}_{2m'-1},\ldots,\phi^{(1)}_2,\ \psi^{(1)}_1,0,0,\ldots,0,0\}$. We can note that the transfer matrix in the bulk is different from that in the boundary layers. But the form of the transfer matrix $T_{4m'\times 4m'}$ in the bulk is the same as that in Eq. (4). Regarding the TMM mentioned above, we know that the most crucial physical quantity is the transfer matrix in the bulk. Thus, we can utilize

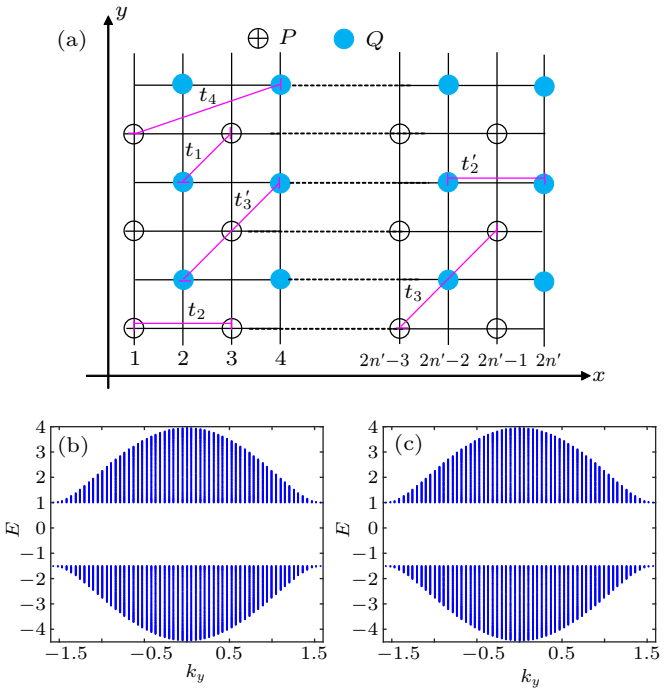


Fig. 2. The schematic illustration of the lattice structure of a finite-size 2D crystal in (a). The energy spectrum of edge modes obtained by the exact diagonalization method (blue dashed line) and TMM (red dashed line) in (b) with $P\leftrightarrow Q$ and (c) with $P\leftrightarrow P$. Here, we only consider the hopping from 1NN CLs and the parameters are $V_P=1.0t_1$ and $V_Q=-1.5t_1$.

the aforementioned TMM to explore edge modes in finite-size crystals with $P \leftrightarrow Q$, except for the boundary conditions, which are different from those of the 1D atomic chain.

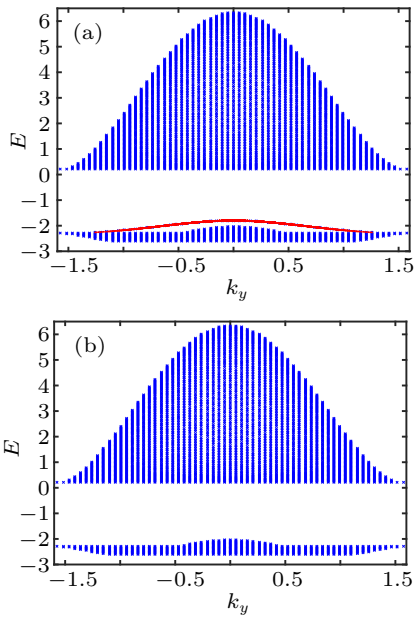


Fig. 3. The dispersion relation of edge modes reached in terms of the exact diagonalization method (blue dashed line) and TMM (red dashed line) in (a) with $P \leftrightarrow Q$ and (b) with $P \leftrightarrow P$. Here, we only discuss the hopping from 1NN to 2NN CLs and the parameters are $t_2 = 0.4t_1$, $t_2' = 0.4t_1$, $t_3 = 0.2t_1$, $t_3' = 0.2t_1$, $V_P = 1.0t_1$ and $V_Q = -1.5t_1$.

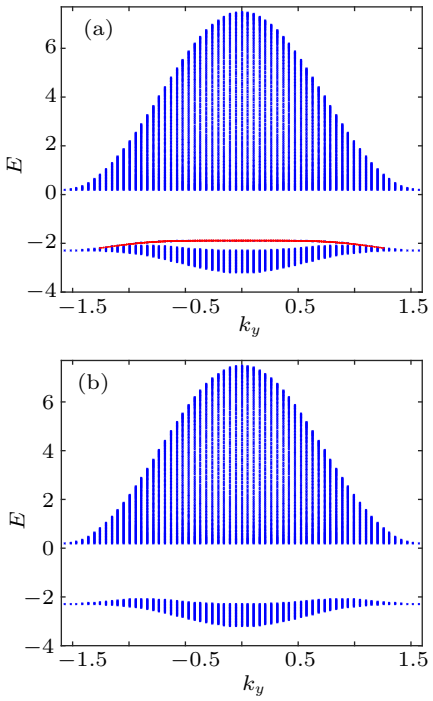


Fig. 4. The dispersion relation of edge modes shown based on the exact diagonalization method (blue dashed line) and TMM (red dashed line) in (a) with $P \leftrightarrow Q$ and (b) with $P \leftrightarrow P$. Here we focus on the hopping from 1NN to 3NN CLs, and the parameters are $t_2 = 0.4t_1$, $t_2' = 0.4t_1$, $t_3 = 0.2t_1$, $t_3' = 0.2t_1$, $t_4 = 0.15t_1$, $V_P = 1.0t_1$ and $V_Q = -1.5t_1$.

To check the correctness of our analytical discussion, we study the behavior of edge modes in the presence of the hopping from 1NN to 2NN (3NN) CLs in detail. Here, we take a 2D square lattice as an example, as shown in Fig. 2(a). With the help of the exact diagonalization method, the behavior of edge modes in the finite-size crystal with $P \leftrightarrow Q$ is found to be consistent with our demonstration, depicted in Fig. 3(a) (Fig. 4(a)). Furthermore, a thorough investigation of such a crystal with $P \leftrightarrow P$ has been conducted, revealing that our analytical calculation aligns well with the numerical findings, illustrated in Fig. 3(b) (Fig. 4(b)).We observe that edge modes can exhibit different behaviors under different edge terminals (see Figs. 3 and 4).

So far, we have presented the conditions for the emergence of edge modes in finite-size crystals with $P \leftrightarrow Q$ and only one electron mode within each CL. Finally, our focus lies on the general case in finite-size crystals with $P \leftrightarrow Q$, where electron modes of each CL are not limited to one and the LR hopping is introduced. In this study, we will not explore this problem further, given the similar treatment to the previous discussion, that is, $m = n = 1$. After a comprehensive consideration, we have come to a similar conclusion about the existence of edge modes for the general case.

4. Model Hamiltonian with $P \Leftrightarrow Q$

In this section, we comprehensively investigate the behavior of edge modes in finite-size systems with $P \Leftrightarrow Q$ in detail. Due to the lack of reflection symmetry in such an infinite crystal, which leads to the asymmetry between the forward and backward transfer matrices from nNN ($n = 2i-1 : i = 1, 2, \ldots, m'$) CLs. Considering the LR coupling, the following QDEs are presented:

$$\begin{cases} E^{(P)}_{n\times n}\Psi_{2i-1} = \sum\limits_{j=1}^{m'}\{F^{(2j-1)}_{n\times m}\Phi_{2i-1+2j-1} \\ \qquad\qquad + F'^{(2j-1)}_{n\times m}\Phi_{2i-1-(2j-1)} + A^{(2j)}_{n\times n}\Delta_{2j}\Psi_{2i-1}\}, \\ E^{(Q)}_{m\times m}\Phi_{2i} = \sum\limits_{j=1}^{m'}\{(F^{(2j-1)}_{n\times m})^{\dagger}\Psi_{2i-(2j-1)} \\ \qquad\qquad + (F'^{(2j-1)}_{n\times m})^{\dagger}\Psi_{2i+2j-1} + B^{(2j)}_{m\times m}\Delta_{2j}\Phi_{2i}\}, \end{cases} \tag{12}$$

here

$$\begin{cases} \Delta_{2j}\Psi_{2i-1} = \Psi_{2i-1-2j} + \Psi_{2i-1+2j}, \\ \Delta_{2j}\Phi_{2i} = \Phi_{2i-2j} + \Phi_{2i+2j}. \end{cases}$$

It has been clearly shown that the form of Eq. (12) differs from that of Eq. (9). The discussion of edge modes in finite crystals with $P \Leftrightarrow Q$ is currently underway. When we take the absolute value of both sides of Eq. (12), it can be verified that the transfer matrix form in the bulk is the same as that in Eq. (11) for the modes in the P and Q CLs, while it differs from that in the boundary layer. It can be reasonably inferred that the existence conditions of edge modes are similar to those obtained in crystals with $P \leftrightarrow Q$. The accuracy of the argument can be verified by generalizing from the specific

case to the general situation in crystals with $P \Leftrightarrow Q$. The initial focus is on the specific scenario where each CL contains an electron mode and the coupling from 1NN CLs is considered. Through a series of derivations, Eq. (12) can be transformed into the following matrix representation:

$$\begin{cases} \left|\Theta_{l+4}^{(P)}\right| = \left|\Theta_{l+2}^{(P)}\right| T'_{2\times2}, \quad \left|\Theta_{l+5}^{(Q)}\right| = \left|\Theta_{l+3}^{(Q)}\right| T'_{2\times2}, \\ \left|\Theta_{3}^{(P)}\right| = |\Omega_0| S'^{(1)}_{2\times2}, \quad \left|\Theta_{4}^{(Q)}\right| = |\Omega_0| \left|\frac{E_1^P}{F_{11}^{(1)}}\right| T'_{2\times2}, \\ l = 1,3,\ldots,2n'-5, \end{cases} \tag{13}$$

where

$$T'_{2\times2} = \begin{pmatrix} b'_1 & 1 \\ -1 & 0 \end{pmatrix}, \quad S'_{2\times2} = \begin{pmatrix} b'_1 + \left|\frac{F'^{(1)}_{11}}{F^{(1)}_{11}}\right| & 1 \\ 0 & 0 \end{pmatrix},$$

$$b'_1 = \left(E_1^P E_1^Q - |F_{11}^{(1)}|^2 - |F'^{(1)}_{11}|^2\right) / |F_{11}^{(1)} F'^{(1)*}_{11}|,$$

$|\Omega_0| = \{|\psi_1^{(1)}|, 0\}$, $|\Theta_{l+4}^{(P)}| = \{|\psi_{l+4}^{(1)}|, |\psi_{l+2}^{(1)}|\}$, $|\Theta_{l+5}^{(Q)}| = \{|\phi_{l+5}^{(1)}|, |\phi_{l+3}^{(1)}|\}$, as well as the form of $T'_{2\times2}$ is akin to that of the transfer matrix in Eq. (11). After detailed discussion, we can draw the corresponding conclusion that there are edge modes. To check the validity of our conclusion, a 2D example with one electron mode within each CL is given in Fig. 5(a). The analytical results have been successfully fitted to the specific hopping parameters, which are consistent with our numerical calculations (see Figs. 5(b) and 5(c)). Second, to enhance the credibility of our analytical results, we also conduct numerical simulations and analytical calculations in detail to investigate the behavior of edge modes when the coupling originates from 1NN to 2NN (3NN) CLs. Notably,

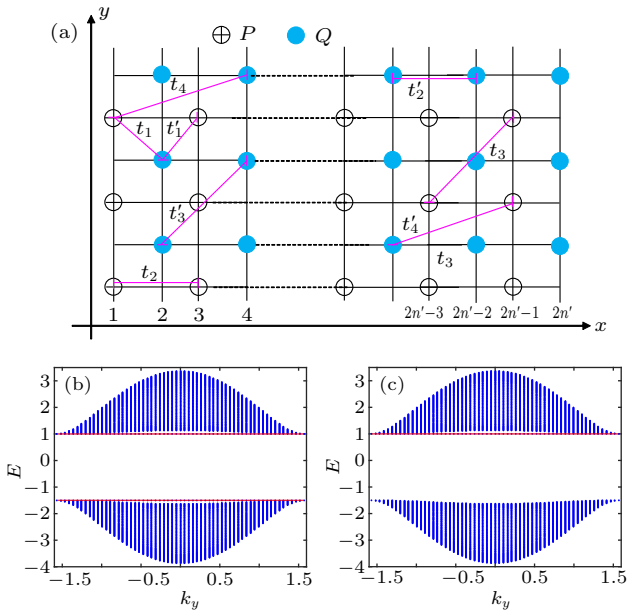


Fig. 5. A schematic illustration of the lattice structure of a finite size 2D crystal in (a) and the dispersion relation of edge modes shown by means of the exact diagonalization method (blue dashed line) and TMM (red dashed line) in (b) with $P \Leftrightarrow Q$ and (c) with $P \Leftrightarrow P$. Here, we only take the hopping from 1NN CLs into consideration and the parameters are $t_1 = 0.7t'_1$, $V_P = 1.0t'_1$ and $V_Q = -1.5t'_1$.

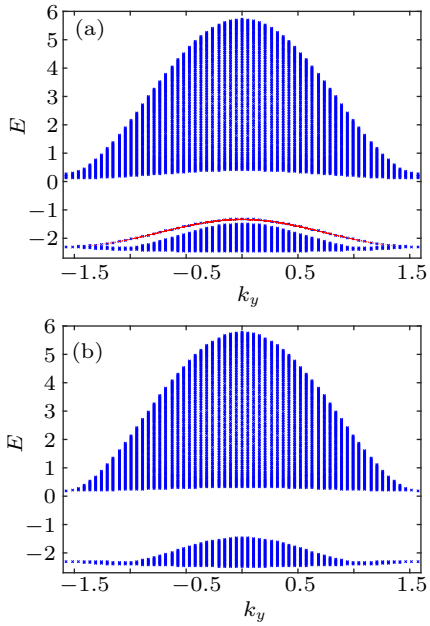


Fig. 6. Band structures obtained by using the exact diagonalization method (blue dashed line) and TMM (red dashed line) in (a) with $P \Leftrightarrow Q$ and (b) with $P \Leftrightarrow P$. Here, we only focus on the hopping from 1NN to 2NN CLs and the parameters are $t_1 = 0.7t'_1$, $t_2 = 0.4t'_1$, $t'_2 = 0.4t'_1$, $t_3 = 0.2t'_1$, $t'_3 = 0.2t'_1$, $V_P = 1.0t'_1$ and $V_Q = -1.5t'_1$.

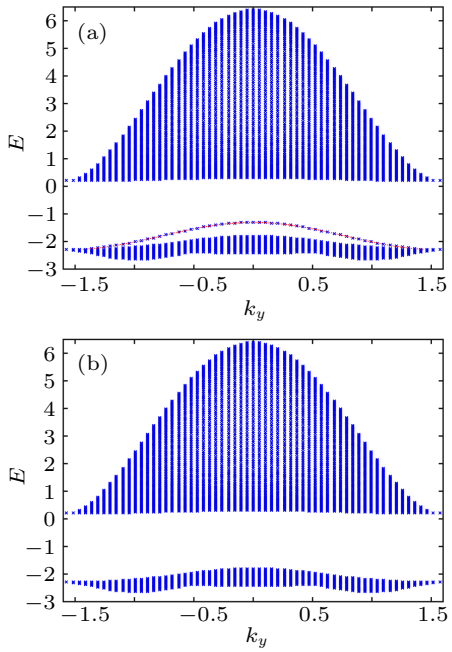


Fig. 7. The dispersion relation of edge modes presented in terms of the exact diagonalization method (blue dashed line) and TMM (red dashed line) in (a) with $P \Leftrightarrow Q$ and (b) with $P \Leftrightarrow P$. Here, we only discuss the hopping from 1NN to 3NN CLs and the parameters are $t_1 = 0.7t'_1$, $t_2 = 0.4t'_1$, $t'_2 = 0.4t'_1$, $t_3 = 0.2t'_1$, $t'_3 = 0.2t'_1$, $t_4 = 0.15t'_1$, $t_4{}' = 0.18t'_1$, $V_P = 1.0t'_1$ and $V_Q = -1.5t'_1$.

a remarkable consistency between these two approaches is observed, illustrated in Figs. 6(a) and 6(b) (Figs. 7(a) and 7(b)). Finally, considering the general case with $P \Leftrightarrow Q$, we can apply the reasoning method used in the general case with $P \leftrightarrow Q$ to derive matrix equations similar to Eq. (11), and subsequently determine the conditions for the existence of edge modes, which are analogous to those in the general case with $P \leftrightarrow Q$. The above discussion is obviously applica-

ble to such finite-size crystals with "*P*–*Q*–*R*–*P*–*Q*–*R*–···–*P*–*Q*–*R*", and so on. Our work provides a way to solve novel edge modes in honeycomb crystalline graphene and transition metal dichalcogenides with different edge terminals.[8,16–24] The conclusions we have reached are also applicable to the 3D and 1D cases, where "lines" correspond to atomic surfaces and points, respectively.

5. Conclusion and perspectives

In this study, we investigate the behavior of edge modes in the presence of different edge terminals and the LR coupling. Based on the lattice model Hamiltonian with the LR hopping, the existence condition of edge modes is determined analytically in systems with different edge terminals by using the TMM. The derived analytical expressions exhibit a wide range of applicability and are independent of the specific choice of hopping parameters. Edge modes can manifest distinct behaviors in crystals with different edge terminals, indicating that the presence of edge modes is intricately linked to the edge configuration. In recent years, due to the remarkable functions and unique properties of different edge configurations in materials, the influence of different edge terminals on edge modes has become an important topic in the field of condensed matter physics, such as honeycomb crystalline graphene and transition metal dichalcogenides, as well as topological crystalline insulators. Our method is suitable for 1D and 3D systems and has the potential to be extended to other finite-size crystals, such as "*P*–*Q*–*R*–*P*–*Q*–*R*–···–*P*–*Q*–*R*". From a more general perspective, our study highlights the effect of the edge in strongly correlated systems.

Acknowledgements

Project supported by the National Natural Science Foundation of China (Grant No. 11847061) and Domestic Visiting Program for Young and Middle-aged Teachers in Shanghai Universities.

References

[1] Von Klitzing K 1986 *Rev. Mod. Phys.* **58** 519
[2] Altland A and Zirnbauer M R 1997 *Phys. Rev. B* **55** 1142
[3] Thouless D J, Kohmoto M, Nightingale M P and den Nijs M 1982 *Phys. Rev. Lett.* **49** 405
[4] Kane C L and Mele E J 2005 *Phys. Rev. Lett.* **95** 226801
[5] Bernevig B A, Hughes T L and Zhang S C 2006 *Science* **314** 1757
[6] Slager R J, Mesaros A, Juričić V and Zaanen J 2013 *Nat. Phys.* **9** 98
[7] Fu L 2011 *Phys. Rev. Lett.* **106** 106802
[8] Pan H and Zhang Y W 2012 *J. Mater. Chem.* **22** 7280
[9] Palacios J, Fernádez-Rossier J, Brey L and Fertig H 2010 *Semicond. Sci. Technol.* **25** 033003
[10] Nakada K, Fujita M, Dresselhaus G and Dresselhaus M S 1996 *Phys. Rev. B* **54** 17954
[11] Fujita M, Wakabayashi K, Nakada K and Kusakabe K 1996 *J. Phys. Soc. Jpn.* **65** 1920
[12] Kunstmann J, Ödoğan C, Quandt A and Fehske H 2011 *Phys. Rev. B* **83** 045414
[13] Kohmoto M and Hasegawa Y 2007 *Phys. Rev. B* **76** 205402
[14] Deng J, Yin Y, Niu H, Ding X, Sun J andMedhekar N V 2017 *Sci. Rep.* **7** 7855
[15] Freeney S E, vanden Broeke J J, Harsveld vander Veen AJ J, Swart I and Morais Smith C 2020 *Phys. Rev. Lett.* **124** 236404
[16] Li Y, Zhou Z, Zhang S and Chen Z 2008 *J. Am. Chem. Soc.* **130** 16739
[17] Jia X, Hofmann M, Meunier V, Sumpter B G, Campos-Delgado J, Romo-Herrera J M, Son H, Hsieh Y P, Reina A, Kong J, Terrones M and Dresselhaus M S 2009 *Science* **323** 1701
[18] Enoki T, Kobayashi Y and Fukui K I 2007 *Int. Rev. Phys. Chem.* **26** 609
[19] Viyuela O, Fu L and Martin-Delgado M A 2019 *ACS Nano* **13** 1635
[20] Ezawa M and Nagaosa N 2013 *Phys. Rev. B* **88** 121401
[21] García-Fuente A, Carrascal D, Ross G and Ferrer J 2023 *Phys. Rev. B* **107** 115403
[22] Sadeghizadeh M, Soltani M and Amini M 2023 *Sci. Rep.* **13** 12844
[23] Salehitaleghani S, Maerkl T, Kowalczyk P J, LeSter M, Wang X, Bian G, Chiang T C and Brown S A 2023 *2D Mater.* **10** 015020
[24] GaoY and Brocks G 2023 *Physica E* **148** 115655
[25] Viyuela O, Fu L and Martin-Delgado M A 2018 *Phys. Rev. Lett.* **120** 017001
[26] DeGottardi W, Thakurathi M, Vishveshwara S and Sen D 2013 *Phys. Rev. B* **88** 165111
[27] Di Liberto M, Malpetti D, Japaridze G I and Morais Smith C 2014 *Phys. Rev. A* **90** 023634
[28] Lepori L, Giuliano D and Paganelli S 2018 *Phys. Rev. B* **97** 041109
[29] Maghrebi M F, Gong Z X and Gorshkov A V 2017 *Phys. Rev. Lett.* **119** 023001
[30] Santos L F, Borgonovi F and Celardo G L 2016 *Phys. Rev. Lett.* **116** 250402
[31] Xu K, Zhang X, Luo K, Yu R, Li D and Zhang H 2021 *Phys. Rev. B* **103** 125411
[32] Wang H P, Ren L, Qin L G and Qiu Y 2020 *J. Phys. Soc. Jpn.* **89** 074705
[33] Wang H P, Ren L, Qin L G and Qiu Y 2021 *Chin. Phys. B* **10** 107301
[34] Lee D H and Joannopoulos J D 1981 *Phys. Rev. B* **23** 4988
[35] Zhao Y Y, Li W and Tao R B 2012 *Physica B* **407** 724
[36] Wang H P and Tao R B 2015 *Chin. Phys. B* **24** 117301
[37] Wang H P, Gao T and Tao R B 2015 *Sci. Rep.* **5** 8679